Tectonophysics, 149 (1988) 245–264
Elsevier Science Publishers B.V., Amsterdam – Printed in The Netherlands

Great Slave Lake Shear Zone, Canadian Shield: reconstructed vertical profile of a crustal-scale fault zone

S. HANMER

Lithosphere and Canadian Shield Division, Geological Survey of Canada, 588 Booth Street, Ottawa, Ont. K1A 0E8 (Canada)

(Received May 29, 1987; revised version accepted November 23, 1987)

Abstract

Hanmer, S., 1988. Great Slave Lake Shear Zone, Canadian Shield: reconstructed vertical profile of a crustal-scale fault zone. *Tectonophysics*, 149: 245–264.

The Great Slave Lake Shear Zone (GSLSZ) of the northwestern Canadian Shield, a 25 km wide, early Proterozoic, transcurrent, dextral, mylonite zone, is a type example of a crustal-scale fault zone profile. With time: (1) the metamorphic grade decreased from granulite to greenschist facies; (2) the locus of high strain narrowed and jumped laterally, abandoning relatively older mylonites. Progressively younger mylonites represent both cooler temperatures and lower pressures; thus the sequence of narrowing mylonite belts represents a series of progressively shallower seated sections through the GSLSZ; (3) deformation evolved through the brittle–ductile transition, initially producing non-dilational penetrative breccias, followed first by discrete non-dilational faulting and subsequently by dilational, quartz "stockworks".

Developing crustal-scale shear zones grow to an optimum width dictated by the requirement of minimum geologically reasonable strain rates for given conditions of wall rock rheology and displacement rate. Independent of variations in relative plate motion, mature shear zones change width and migrate laterally as a function of inferred thermally activated rheological changes within the wall rocks.

Introduction

A decade has now passed since the publication of Sibson's (1977) seminal description of the downward widening profile of a model crustal-scale shear zone in continental crust (Fig. 1). Grocott (1977) has already drawn attention to the potential of deeply excavated shear zones in Precambrian terranes as analogues for the aseismic levels of modern large-scale faults such as the San Andreas Fault. Yet few natural examples of transcurrent shear zones which embody the various elements of the model have been identified (Bak et al., 1975b; Grocott, 1977), let alone documented in detail (Bak et al., 1975a). Indeed, Sibson (1983) has pointed out that there are two further models for major shear zones which warrant consideration; constant width or decoupling with depth (see also Lachenbruch and Sass, 1980).

The purpose of this paper is to establish that the circa 2.0 Ga vertical, transcurrent, Great Slave Lake Shear Zone (GSLSZ) of the northwestern Canadian Shield (Figs. 2 and 3), comparable in width (25 km) with the widest documented mylonite zones in the world to date (e.g. Grocott, 1977, 1979a,b), is a type example of Sibson's crustal-scale model transcurrent fault profile. First, field evidence will be presented for a sequential decrease in metamorphic grade and width of the active part of the mylonite belt. It will then be suggested that the narrower, cooler mylonite belts represent horizontal sections of shallower structural level through a fault profile, compared with the wider, hotter belts. Third, this hypothesis will

0040-1951/88/$03.50

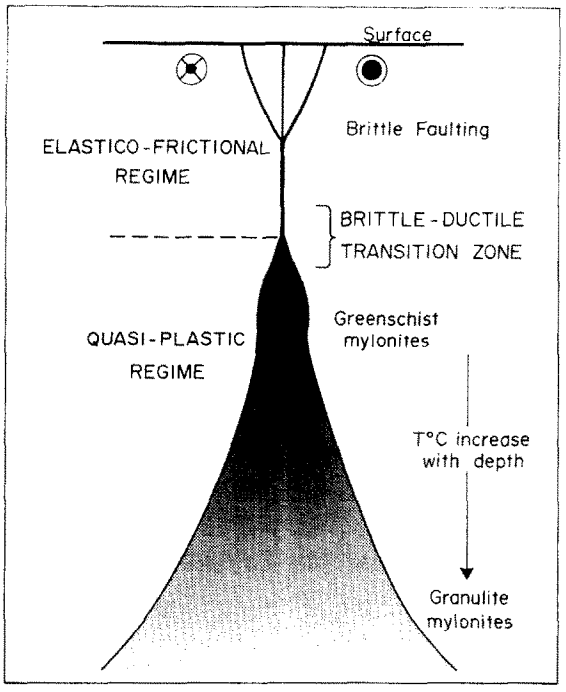

Fig. 1. Schematic vertical "fault profile" through an idealized crustal-scale transcurrent shear zone (after Sibson, 1977; see also Sibson, 1979, 1982, 1983, 1986). Dotted circle advancing towards, crossed circle receding from the viewer. Discussed in text.

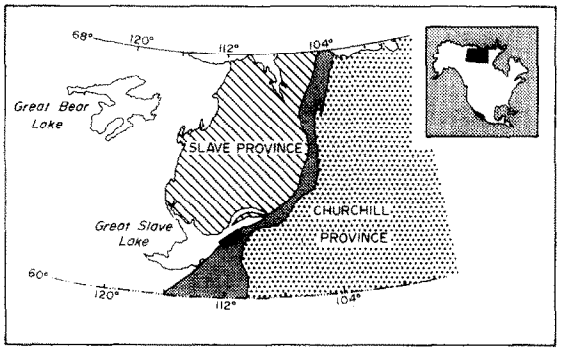

Fig. 2. Disposition of the structural boundary between Slave and Churchill provinces in the northwestern Canadian Shield. The finely stippled band, largely drawn from the magnetic anomaly pattern (Geological Survey of Canada, 1964a, b) is, in the north, the Thelon Tectonic Zone (Thompson et al., 1985) and, in the south, the Taltson magmatic Zone (Bostock et al., 1987), linked and dextrally offset by the NE–SW-trending Great Slave Lake Shear Zone (Hoffman, 1987; see Figs. 3 and 5). Black rectangle marks location of study area.

be tested by geothermobarometry. Finally, some of the controls of shear zone width in developing and mature crustal-scale fault zones, highlighted by this study, will be discussed.

In this paper, two useful adjectives are used in macroscopic descriptions of mylonitic rocks. "Homoclastic" applies where more than 2/3 by volume of the porphyroclast population of a mylonitic rock constitutes a dominant size class. "Heteroclastic" is used where the frequency of porphyroclast size is perceptibly spread across the size range (see Hanmer, 1987).

Shear zones in profile

Sibson's model fault profile invokes a rheologically layered crust; an upper elastic-frictional layer and a lower quasi-plastic layer (Fig. 1). The two layers, more appropriately referred to as rheological regimes, are separated by a brittle–ductile transition zone of complex definition. The complexity reflects the different sensitivities of the stress–strain rate relationship of the different mineral species to depth-related environmental factors such as temperature and lithostatic pressure, as well as to strain rate itself (e.g. Tullis and Yund, 1977, 1980).

If one considers only the ductile rheological regime, Sibson's model describes a progressive increase in width of the shear zone profile with depth. The narrowest part of the profile corresponds to the level in the crust where quartz begins to deform significantly by dislocation creep. This occurs under conditions corresponding to the chlorite zone of the greenschist facies and is expressed as narrow (circa 1 km) mylonite to ultramylonite zones. The width of the mylonite zone is principally a function of two factors: (1) the thermally controlled stiffness of the wall rocks; and (2) the mechanically induced strain-softening within the shear zone (Watterson, 1975; White, 1976; Poirier and Guillopé, 1979; White et al., 1980) due to the dynamic microstructural changes brought about by the development of the fine-grained mylonite (Bell and Etheridge, 1973). Strain-softening may be enhanced by reaction-softening (White and Knipe, 1978; Williams and Dixon, 1982). In terms of energy expended, it is

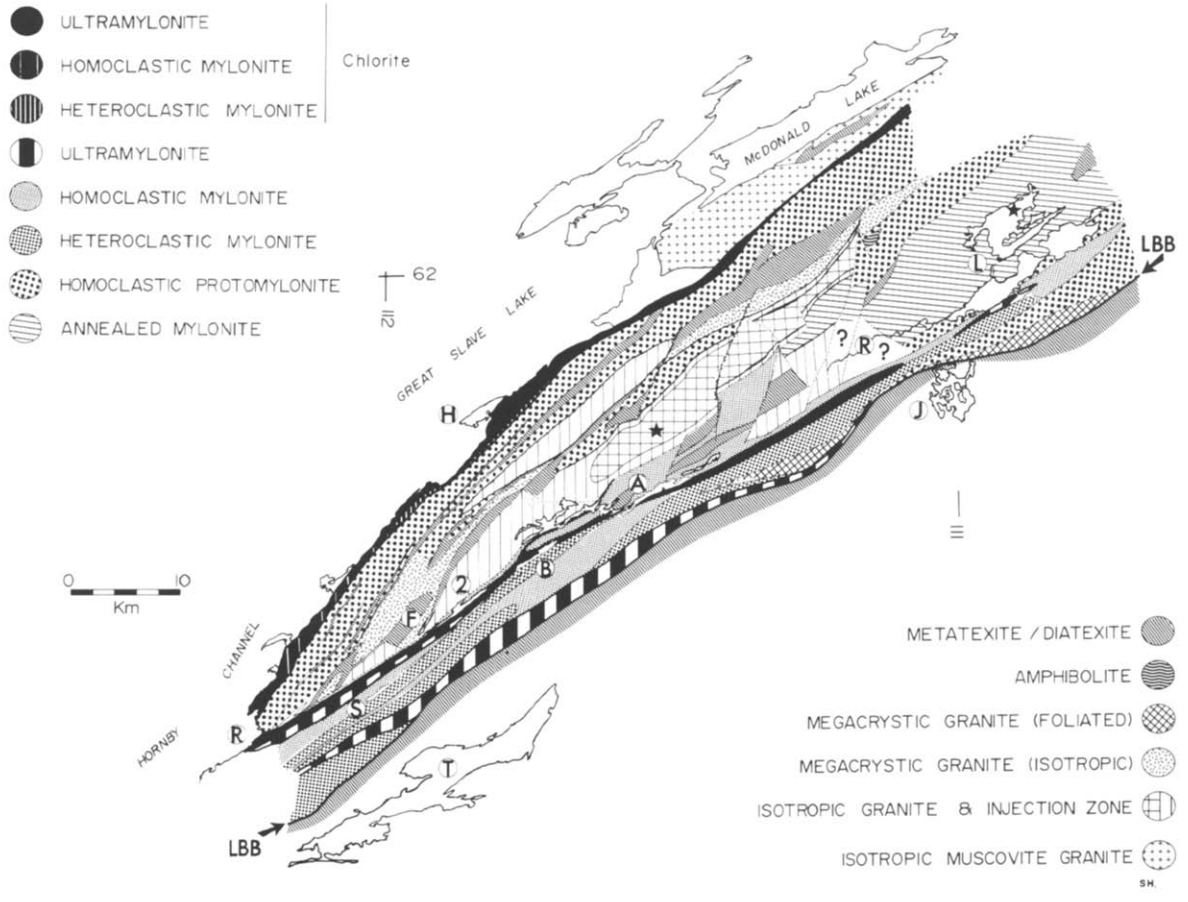

Fig. 3. Map showing mylonites and other lithologies in Great Slave Lake Shear Zone. Lakes are Avocado (*A*), Barrier (*B*), Falls (*F*), Jigsaw (*J*), Laloche (*L*), Spike (*S*), Second (*2*), Thubun (*T*). Other names are Hook Point (*H*) and Laloche River (*R*). The heavy solid line (*LLB*) is the southeast boundary of the Laloche batholith. Stars mark geochronology sample sites mentioned in text. Discussed in text.

more efficient to accommodate the displacement of two blocks of cold, stiff wall-rock by high magnitude ductile strain in a narrow zone of soft material than to accommodate the same displacement by lower magnitude strain in a wider zone of stiff wall rock (Watterson, 1975). Since ambient metamorphic grade and temperature generally increase with depth, the thermal softening of the wall rocks decreases the potential for mechanically induced rheological contrast between wall rock and shear zone rock. This in turn reduces the advantage of narrow over wide deformation zones. Thus the width of the fault profile increases with depth. It follows that during syntectonic cooling, either isobaric or with accompanying uplift, the locus of active deformation in crustal-scale shear zones should progressively narrow, abandoning once active parts of the shear zone.

Great Slave Lake Shear Zone

Faults and mylonites have long been known on the southeastern side of Great Slave Lake (Stockwell, 1982; Henderson, 1939; Wright, 1951, 1952; Hoffman et al., 1977). Reinhardt (1969) was the first to appreciate the extent of the mylonites, but did not map them. Profiting from Reinhardt's work, an excellent aeromagnetic data base (Geological Survey of Canada, 1964a,b, 1984) and good outcrop, recent mapping at 1 : 25,000 to 1 : 50,000 scales has documented the distribution, time and kinematic relations of a wide zone of mylonites.

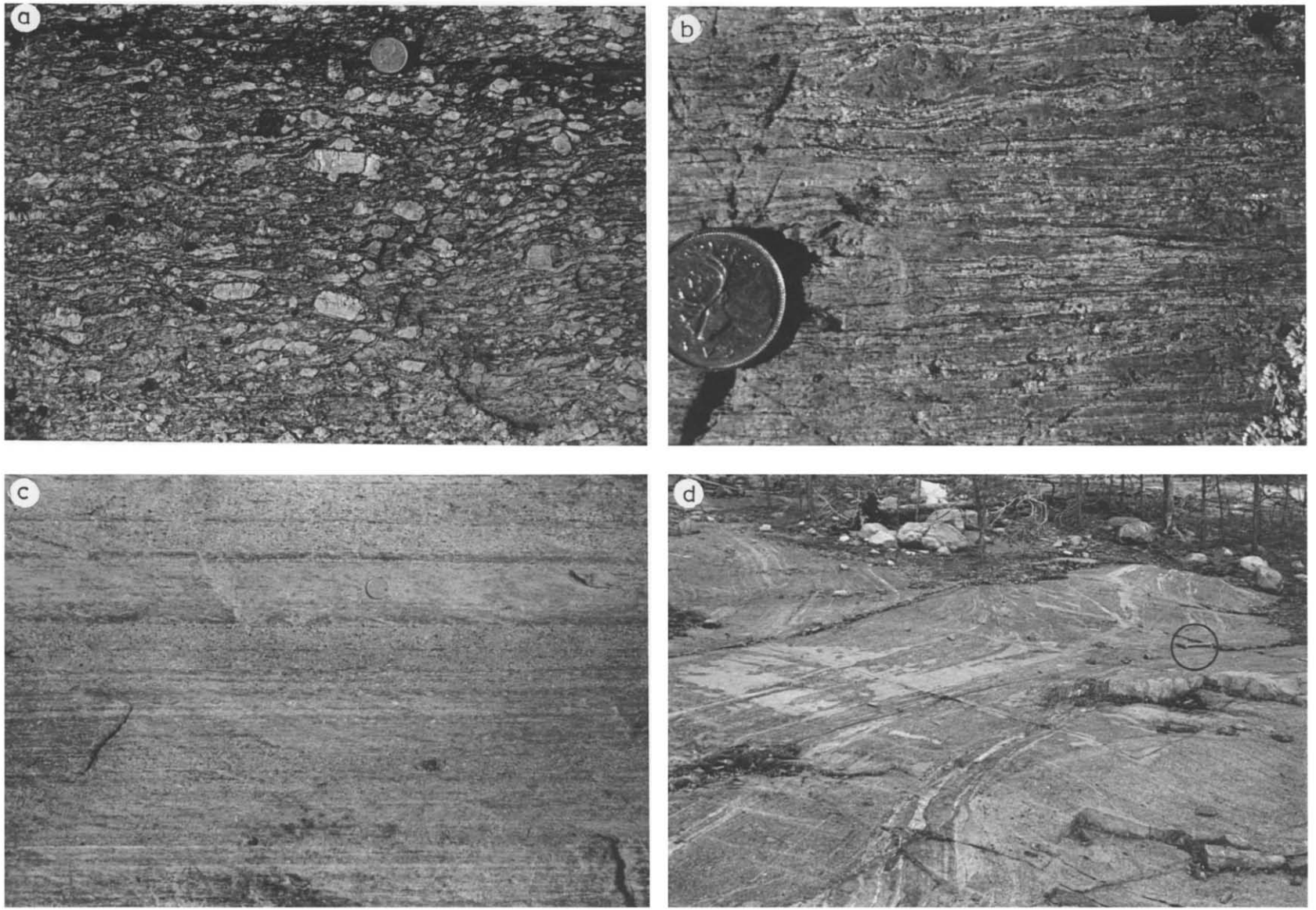

Fig. 4. Aspects of mylonitization in Great Slave Lake Shear Zone. Coin scale = 23 mm. a. Well foliated megacrystic granite (Laloche batholith), parent to mylonites. b. Well developed heteroclastic ribbon mylonite derived from A. Note K-feldspar (medium grey), plagioclase (light grey) and quartz ribbons (dark grey) plus large K-feldspar porphyroclast (top centre). c. Very straight layering in mylonitized granitoid. Dark spots are plagioclase porphycroclasts in granodioritic homoclastic mylonite to protomylonite. Featureless bands (e.g. at coin) are granitic fine homoclastic mylonite. d. Disrupted annealed granoblastic mylonite in belt #1. Note three pods (top left, top right and bottom-right) with internal mylonite layering discordant to bounding mylonite which separates them. Hammer (circled) for scale.

They comprise the Great Slave Lake Shear Zone (GSLSZ), an early Proterozoic dextral transcurrent mylonite zone, up to 25 km wide (Hanmer and Lucas, 1985). The mylonites of the GSLSZ were derived at the expense of a syntectonic granitoid batholith, with which the shear zone is spatially coincident (Hanmer and Connelly, 1986). More recently, it has been proposed that the GSLSZ is a continental transform fault which accommodated eastward motion of the Slave Craton as it impinged upon the western margin of the Churchill Province (Fig. 2) during the Lower Proterozoic (Hoffman et al., 1986; Hoffman, 1987).

Protolith: Laloche batholith

The GSLSZ is a corridor of five mylonite belts (Figs. 3 and 4), in large part derived by the deformation of the megacrystic Laloche batholith. The batholith is a leucocratic biotite–hornblende granitic to tonalitic (Streckeisen, 1976) early Proterozoic intrusion (circa 2.0–1.92 Ga, U/Pb in zircon; Bowring pers. commun., 1987). It extends NE–SW across and beyond the map area (Fig. 3). Its northwestern boundary is now marked by a chlorite-bearing mylonite belt along the shoreline of Great Slave Lake, while its southeastern contact extends from near Thubun Lakes to near Laloche Lakes (Fig. 3). Few individual plutons can be distinguished within the batholith. The most obvious are the elongate bodies of young isotropic equigranular or megacrystic granite emplaced between Great Slave Lake and the Laloche River (Fig. 3). The internal structure of the older deformed parts of the batholith is reflected in the distribution of very large, continuous (0.5–3.0 by 50 km), screens of paragneiss. Progressive sheeted contacts between the granitoid and the paragneisses are intrusive. The screens are so large that they probably represent curtains of country rock caught between plutons, or roof pendants protruding down into the batholith. The paragneiss screens are very common, except to the SE of the Laloche River, where they are very rare (Fig. 3). Comparison of Figures 3 and 5 shows a clear spatial coincidence between the lithological structure of the batholith and the distribution of the mylonite belts of the GSLSZ, which will be further discussed below.

The batholith is visibly intrusive with respect to the sillimanite–cordierite–garnet granites and migmatitic paragneiss (Bostock, 1982, 1987) of the Churchill Province to the southeast. Focusing on the extensively exposed southeastern side of the batholith; to the northwest of the contact zone the mylonites are uniformly pink and of granitic composition. On the southeastern side they are pink, dark grey or white, in alternating strips. The lithological contact is a zone of progressively increasing intercalation of grey and white mylonite within the pink, wherein the grey and white mylonites become volumetrically dominant towards the southeast. Further to the southeast the mylonitic foliation becomes progressively weaker and the compositional layering becomes more irregular. Within approximately a kilometre of the limit of the predominantly pink mylonites, the gneiss is a highly contorted, grey and white sillimanite–cordierite–garnet mature metatexite to diatexite (Mehnert, 1968; Brown, 1973), with no pink granitoid. The sheeted zone of mixed lithologies is the mylonitized, intrusive contact of the Laloche batholith, emplaced into undated upper amphibolite facies migmatitic paragneiss. Presumably, the batholith was also intruded into the muscovite–sillimanite bearing archean granites (Reinhardt, 1969; Hanmer and Lucas, 1985) of the Slave Craton to the northwest although this relationship is now obscured by deformation (Fig. 3).

Mylonite belts

Geometry and kinematics

The mylonite belts are referred to, in chronological order, as belts #1, #2, #3 and the Laloche River and Hornby Channel ultramylonite belts (Fig. 5). The belts preserve mineral assemblages of the granulite (#1), upper amphibolite (#2), lower amphibolite (#3) and greenschist facies (Laloche River and Hornby Channel belts). Mylonitic foliation and lithological layering are steeply dipping to vertical and strike NE–SW (Fig. 6a). A widely developed extension lineation is generally subhorizontal, with the striking exception of a central

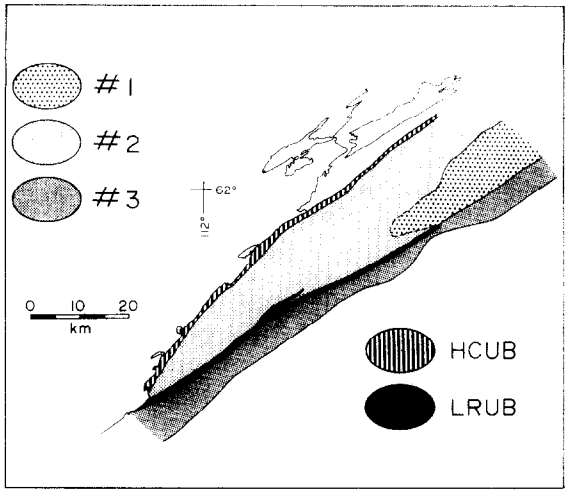

Fig. 5. Division of Great Slave Lake Shear Zone into belts #1, #2, #3 plus the Laloche River (LRUB) and Hornby Channel (HCUB) ultramylonite belts. Discussed in text.

corridor bordering the northwest side of belt #3 (Fig. 6b; see below). The alignment of individual mineral grains (sillimanite, biotite, hornblende) and quartzo-feldspathic aggregates, the presence of boudinage, plus the alignment of isoclinal fold axes, combine to indicate that this is a true extension lineation. A widespread suite of mechanically independent shear criteria, such as rotated stiff inclusions and porphyroclasts (Hanmer, 1984; Passchier and Simpson, 1986), shear band foliation (White et al., 1980), asymmetrical pull-aparts of all types (Hanmer, 1986), "C and S" planes (Berthé et al., 1979), rotated fold axial planes (Hanmer, 1984; Murphy, 1987), asymmetrical pressure shadows (Durney and Ramsay, 1973), indicates a consistent dextral shear along the lineation direction throughout the ductile history of the GSLSZ. Detailed descriptions of the field aspects of the kinematic indicators and the mylonitic fabrics are given elsewhere (Hanmer, 1984, 1986, 1987; Hanmer and Lucas, 1985). Brief descriptions of the mylonite belts, in order of decreasing metamorphic grade, are given here.

Granulite facies

In belt #1 metapelites carry the assemblage garnet–sillimanite–cordierite–biotite–plagioclase–K feldspar–quartz plus melt. Garnet–orthopyroxene–biotite–plagioclase–K feldspar–quartz occurs in metagranitoids and mylonites derived from them. Amphibolites are locally two pyroxene bearing or garnetiferous. At both the outcrop and map scales, the mylonites of this belt, up to 10 km wide, are the most complex in the GSLSZ. Rectilinear, banded, annealed granoblastic mylonites, or "straight gneisses" (Myers, 1978, 1984; Davidson, 1984; Coward, 1984; Hanmer, 1987), can be traced back into very coarse-grained protoliths. Microstructural relationships, such as the alignment in the foliation and lineation of sillimanite and biotite, orthopyroxene trails drawn out along the foliation, and garnet augen in the foliation, indicate that the mylonites formed under granulite facies conditions.

The mylonites have been tectonically disrupted at all scales from 10's to 1000's of metres by a combination of folding, shearing and the emplacement of cross-cutting leucogranite (Fig. 4D). Folding of the mylonites and further shearing along the fold limbs has resulted in shear-bound pods with NW–SE striking internal foliation and rectilinear layering, enclosed by generally NE–SW striking, upright zones, 10's to 100's of metres wide, of further shearing. Elsewhere, stiff blocks have rotated between adjacent shears. Veins of isotropic leucogranite, cross-cutting within the shear-bound pods, are deformed and transposed within the bounding shear zones. Briefly stated, widespread rectilinear mylonites were developed during the initial stage of the deformation. At a later stage, either during or after emplacement of the swarm of leucogranite veins, the earlier formed tectonites were disrupted by heterogeneous strain. This relationship will be used later to show that the disruption of the rectilinear mylonites was due to continued post-granulite movement in the adjacent belts #2 and #3.

Amphibolite facies

In belt #2, the metapelites carry the assemblage garnet–sillimanite–cordierite–biotite–plagioclase–K feldspar–quartz and amphibolites are locally garnetiferous. In belt #3, the metapelites carry the assemblage garnet–sillimanite–white mica–biotite–plagioclase–K feldspar–quartz.

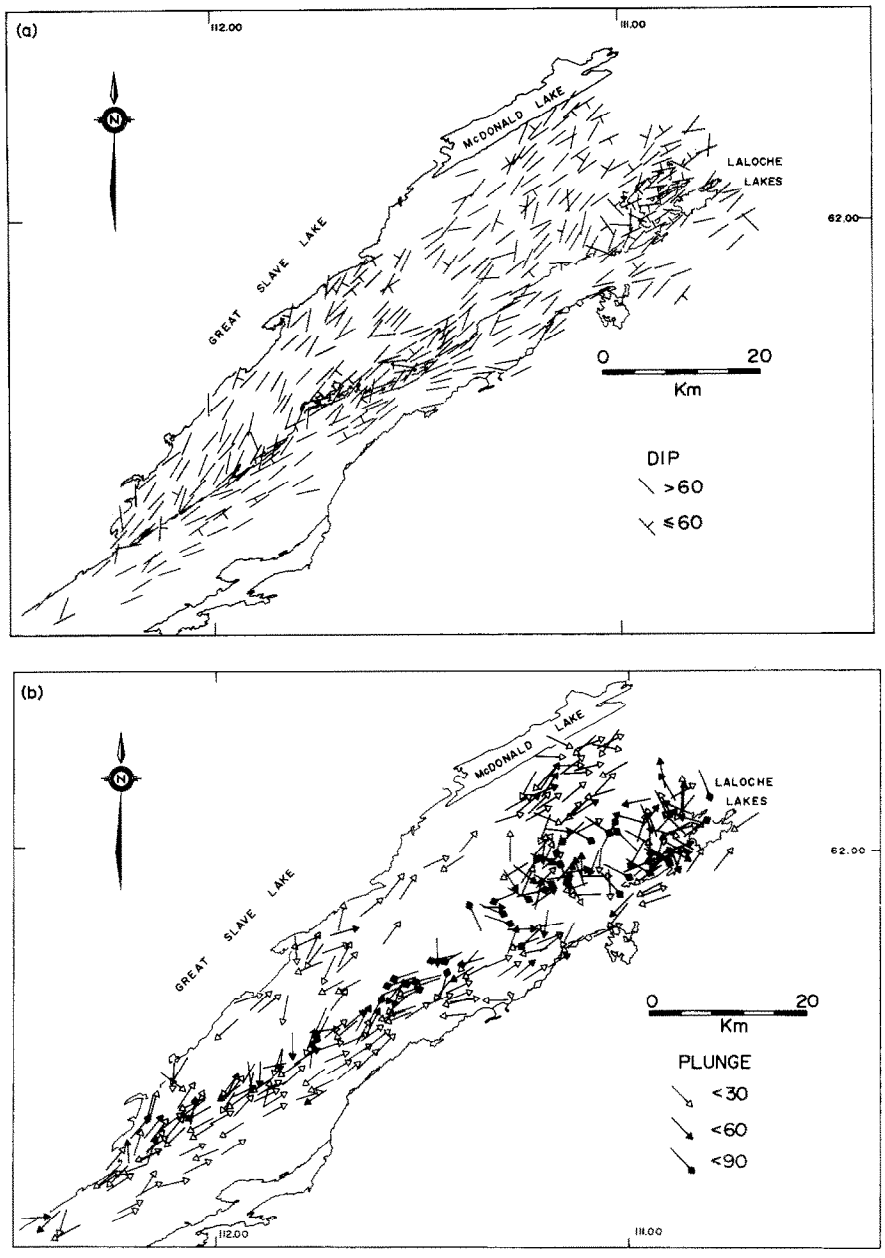

Fig. 6. a. Maps showing foliation and layering in Great Slave Lake Shear Zone. Only two dip classes are represented, for clarity. Note variable dips and strikes in the disrupted annealed granoblastic mylonite of belt #1 in the Laloche Lakes area. b. Lineation orientation in Great Slave Lake Shear Zone. For clarity, only three plunge classes are shown. Note the corridor of *mixed steep and shallow* plunges extending southwest from the Laloche Lakes area. They occur within mylonites of all metamorphic grades present in GSLSZ, and hence are spatially rather than temporally controlled. Discussed in text.

These are belts of homogeneous ribbon mylonites. However, they are not uncommonly compositionally banded on a decimetre scale, i.e. grey–pink granodioritic mylonite, with a somewhat greater plagioclase and biotite content, alternating with the pink granitic mylonite. Belt #2 is up to 10 km wide and is dominated by finely homoclastic protomylonites, in which the feldspar porphyroclasts are small, well rounded and remarkably constant in size (1–2 mm in diameter). They are visibly

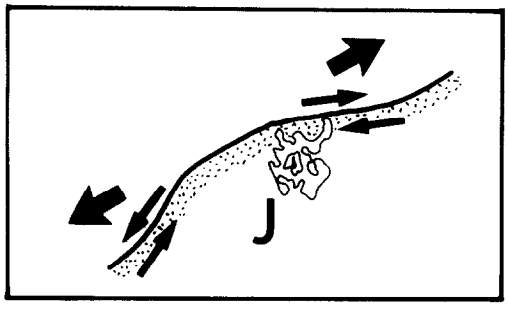

Fig. 7. Schematic illustration of sense and orientation of shearing on either side of the constriction of belt #3 in the Jigsaw Lake (*J*) area to show the relationship between regional dextral shear, local sinistral shear and extension along the Great Slave Lake Shear Zone direction. Wall rock outside of shear zone is stippled.

derived by the mechanical degradation of large (2–6 cm) feldspars of a megacrystic granite precursor, locally preserved in widespread, small, low-strain pods. The protomylonites commonly pass into mylonites, locally to ultramylonites. Homoclastic mylonite predominates on the SE side of the belt, north of Avocado Lake (Fig. 3).

Belt #3 is 5 km wide and consists mainly of heteroclastic and homoclastic mylonites. The northwest and southeast flanks of the belt are marked by two continuous ultramylonite belts, up to 2 km wide by up to 70 km long (Fig. 3). The ultramylonites of this belt are biotite bearing and quite distinct from the chlorite-bearing ultramylonites of the adjacent Laloche River belt. Belt #3 as a whole is very straight and of constant width, except for a constriction just west of Jigsaw lake where it narrows to about 2 km (Figs. 3 and 7). Shear sense criteria are all sinistral in the southwestern part of the constriction. This is the only significant exception to the dextral shear sense of the GSLSZ and suggests that the constriction is the result of anomalously strong subhorizontal NE–SW extension of this part of belt #3.

Greenschist facies

The Laloche River and Hornby Channel ultramylonite belts are characterized by the assemblage chlorite–white mica–albite–epidote ± quartz. These two chlorite-bearing belts are identical in every way. They are 1.0–1.5 km wide and comprise monotonous dark green to white, fissile ultramylonite to heteroclastic mylonite with an ultrafine matrix. Locally, a flinty non-fissile variant occurs. All mylonite types are cut by a 500 m wide zone of pervasive non-disruptive breccias, characterized by minimal dilation as evidenced by the absence of visible introduced quartz or calcite (Fig. 8a). The breccia is cut by discrete E–W vertical fault planes, spaced at metre intervals. Dextral motion on the faults results in an anticlockwise rotation of both the fault planes and the layering preserved in the breccias. Pseudotachylite veins cross-cut both faults and breccias (Fig. 8b) and are also present in the adjacent ultramylonites of belt #3. Unequivocal generation surfaces (e.g. Grocott, 1981) have not been documented. All of these tectonites and structures are cut by subconcordant vertical quartz veins ("stockworks"), 25 m wide by up to 40 km long.

There are no metamorphic gradients or isograds preserved within the GSLSZ. The following field relationships demonstrate that the higher grade metamorphic assemblages are older than the lower grade ones.

(1) The granulite mylonites of belt #1 are cross-cut by a network of veins of coarse, isotropic leucogranite, each up to several metres in width. The passage from belt #1 to the flanking belts #2 and #3 is marked by deformation of the granite veins, which leads to their complete transposition within the latter two belts. Hence the belt #1 mylonites are the oldest preserved tectonites of the GSLSZ. The granite veins are the same as those shown above to be pre- or syntectonic with respect to the disruption of the granulite facies of belt #1. This shows that the disruption is coeval with, and perhaps due to, continued movement in the flanking post-belt #1 mylonites.

(2) Since belts #2 and #3 are separated from one another by the chlorite-bearing ultramylonites of the Laloche River belt (Fig. 3), their time relationship must be indirectly deduced. (a) As just shown, the mylonites of both belts are younger than those of belt #1. (b) Their respective metamorphic mineral assemblages are aligned in the foliations and lineations and indicate the conditions of deformation in each belt. (c) The belts are

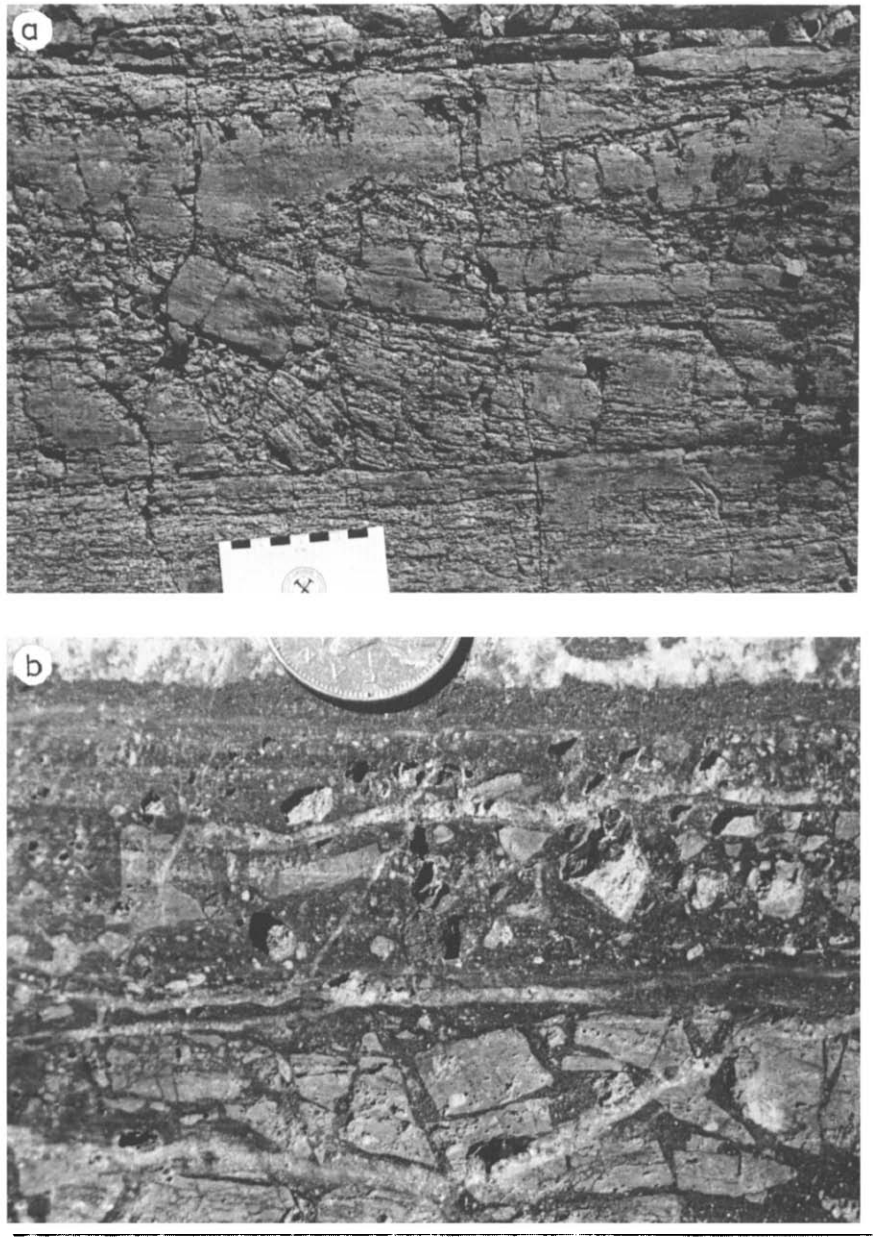

Fig. 8. Brittle deformation in greenschist mylonite belts. a. Ultramylonite disrupted by non-dilational, penetrative brecciation. Note absence of introduced material. Scale bar in 1 cm increments. b. Injection of pseudotachylite (dark grey) into strongly dilated ultramylonite.

metamorphically monotonous over strike lengths in excess of 100 km. These observations suggest that the lower amphibolite facies mylonitization and metamorphism preserved in belt #3 is younger than the deformation and metamorphism preserved in the nearby upper amphibolite facies belt #2.

An alternative hypothesis would require that differential movement of well over 100 km along the intervening Laloche River belt resulted in the juxtaposition of coeval tectonites of different metamorphic grade. Three observations militate against this hypothesis. (a) The termination of the Laloche River ultramylonite belt within the map

area does not favour accommodation of such a large displacement by the ultramylonites (Fig. 3). (b) From the consistent curvature of widespread, non-dilational, "Z"-shaped en-echelon sigmoid fractures (Ramsay and Graham, 1970), Hanmer and Connelly (1986) calculate that the Laloche River belt breccias have only accommodated displacement of the order of a few kilometres at the very most. (c) The largest of the late quartz stockworks runs northeastward from Spike Lake in belt #3, crosses into the Laloche River belt at Avocado Lake and continues along the chlorite ultramylonites for several kilometres to the northeast of the lake. The vein does not offset the Laloche River belt–belt #3 boundary (Fig. 3) and thus probably represents a late dilational fracture rather than an important transcurrent structure.

(3) The amphibolite facies mylonites of belts #2 and #3 can be traced continuously into the chlorite-bearing ultramylonites of the Laloche River belt and Hornby Channel belt. Progressive mechanical destruction of the higher grade mylonites and their minor structures, such as folds, boudins and porphyroclasts, visibly accompanies retrogression of garnet, biotite and sillimanite to chlorite and white mica. Furthermore, the structural trends in belt #2 are visibly truncated at the map scale by the two chlorite-bearing belts (Fig. 3). While these observations demonstrate that the Laloche River belt and Hornby Channel belt are younger than the mylonites which they rework, the age relationship of the Laloche River belt with respect to the Hornby Channel belt remains unconstrained.

Time range

The oldest granitic material in the GSLSZ is a uniformly biotite-rich megacrystic metagranitoid which forms much of the mylonite precursor in belt #1. It cannot be determined whether this rather sombre granitoid was emplaced syn- or pretectonically with respect to mylonitization. Uranium-rich zircons yield a preliminary age of circa 1.98 Ga (Bowring, pers. commun., 1987).

The youngest granitoids are represented by two separate bodies which occupy a significant area within belt #2. The larger of the two is a vertical sheet-like body of isotropic to poorly foliated coarse equigranular granitoid, surrounded by a kilometre wide injection zone of thick (10's of metres) veins of the same granitoid cutting across granitic mylonite of the country rock envelope. The broad "V"-shaped outcrop of the injection zone, in the Barrier Lake–Second Lake area, along strike from the main granitoid outcrop (Fig. 3), implies that the roof of the pluton is arch-shaped and plunges gently towards the southwest. The injection zone is clearly syntectonic with respect to the chlorite-bearing ultramylonites of the Laloche River belt since (i) veins of the equigranular granitoid cut the ultramylonites, but are themselves only mildly foliated to protomylonitic, and (ii) the injection zone is cut by regionally concordant, narrow (< 10 m) chlorite-bearing mylonite zones. Equigranular granitoid from north of Avocado Lake (Fig. 3) yields a preliminary age of circa 1.925 Ga (Bowring, pers. commun., 1987).

Structural synthesis

It is appropriate here to summarize the structural history arising from the foregoing data, in order to provide a context for the geothermobarometry described below. At the presently exhumed deepest crustal level, the GSLSZ initially developed as a wide, dextral, transcurrent, granulite facies mylonite zone. Since no relics of these early mylonites have been observed within the flanking younger mylonites, its maximum width remains indeterminate (> 10 km, possibly 25 km). With time, the ambient temperature at the structural level of the presently exposed granulite mylonites decreased. It is reasonable to assume that decreasing efficiency of temperature-sensitive, grain-size independent strain mechanisms, such as dislocation glide and climb (e.g. Nicolas and Poirier, 1976; Poirier, 1985), led to stiffening of the wall rocks. The potential for softening associated with grain-size reduction was enhanced, and deformation began to concentrate in narrower, cooler mylonite belts. A part of the older granulite mylonites in which the strain rate decayed (belt #1), and which began to behave as a stiff island within the shear zone, was thus abandoned. High strains were concentrated in the 15 km aggregate

width of the rest of the shear zone (belts #2 and #3) until, with further cooling and stiffening of the wall rocks, the dextral displacement of the wall rocks past each other was most efficiently accommodated by deformation within an even narrower mylonite zone. This resulted in deformation abandoning the upper amphibolite facies mylonites in that part of the batholith with the large screens of paragneiss (belt #2), and concentration of high strain in the inclusion-poor granitoid mylonites of what is now the lower amphibolite facies belt #3.

The following alternative scenario warrants discussion. On abandoning the present belt #1, the new locus of high strain could have lain entirely within what is now belt #2. The present belt #3 would have constituted part of the southeastern wall rock to the shear zone at this time. Subsequently, the locus of high strain would have jumped out of the old shear zone into a newly initiated zone lying entirely within the extremely coarse, "stiff" non-mylonitized wall rock (belt #3). By yet further coincidence, the southeastern margin of this new shear zone would be marked by a lithological boundary of the same batholith, whose northwestern contact marks the limit of the belt #2 mylonites (Fig. 5). It is rheologically unreasonable to favour initiation of ductile deformation in a coarse megacrystic granite over continued deformation in a fine-grained, strain-softened granitic mylonite under lower amphibolite facies conditions; hence this alternative scenario can be reasonably discarded.

With further cooling and stiffening of the wall rocks, belt #3 was abandoned and the zone of high strain was confined to two belts of chlorite-bearing mylonite, each approximately one kilometre wide. The deformation was sited in the Laloche River belt, at the lithological contact between inclusion-poor and inclusion-laden granitoid, and in the Hornby Channel belt at the northwest contact of the batholith.

The central corridor of mixed steeply and shallowly plunging extension lineations (Fig. 6b) present a kinematic anomaly within the transcurrent GSLSZ. Careful observation shows that the slip vector is locally parallel or locally normal to the steep extension lineation. Where it is parallel, the slip vector shows either southeast side up or down. The widest part of the corridor occurs within the disrupted, heterogeneously deformed granulites of belt #1. To the southwest, the corridor lies mostly within the upper amphibolite mylonites and paragneiss of belt #2, but also within the greenschist ultramylonites of the Laloche River belt. In the former, there are local indications of heterogeneous deformation, mostly in the form of 50–100 m wide pods or nests of 1–10 m wavelength folds deforming the mylonitic foliation, which are wrapped-around by the external mylonitic foliation. In the Laloche River belt, although much of the ultramylonite has been subsequently reoriented by brittle faulting, mixed lineations are seen where the vertical foliation strikes 060, i.e. is undisturbed.

It is emphasized that (1) the mixed lineations are synmetamorphic with respect to the disruption of the belt #1 annealed granoblastic mylonites, the belt #2 mylonites and those of the Laloche River belt, i.e. the mixed lineations are spatially rather than temporally controlled. (2) They are developed in a corridor of heterogeneous strain within which elliptical relatively stiff pods of lower strain are separated from each other by anastomosing higher strain bands. (3) The corridor is most extensively developed in the drier, stronger granulite facies tectonites and is least pronounced in the more hydrous greenschist facies tectonites. (4) The corridor is located along a bulk compositional boundary along the line of the Laloche River. Therefore, I suggest that the compositional boundary represents a rheological interface within the Laloche batholith and that the heterogeneous deformation (Bell, 1981) on its northwestern side is a result of strain incompatibilities across that interface. The steep lineations would have formed as a result of local shortening across the flow plane (transpression; Sanderson and Marchini, 1984) as elliptical pods of relatively stiff material attempted to move past each other. Such movement may have been lateral, or vertical where convergence of two pods displaced a third one caught between them. If this suggestion is reasonable, then the main plutonic architecture of the batholith was in place even during the high grade early history of the GSLSZ.

Deformation in both chlorite mylonite belts passed from the ductile to the brittle regime. Given the hardening effect of pressure in the brittle regime (e.g. Paterson, 1978, pp. 178–181), the evolution with time from initial penetrative, non-dilational brecciation, via spaced asymmetric en-echelon fault arrays to quartz veins 10's of kilometres in length, strongly suggests a progressive decrease of effective confining pressure. This could represent a decrease in lithostatic pressure due to erosional unroofing and/or an increase in pore fluid pressure. This raises the question as to whether the cooling during the ductile history of the GSLSZ was itself isobaric or associated with significant uplift.

Geothermobarometry

If the GSLSZ is truly an example of a sequence of preserved horizontal sections through the crustal-scale profile of an active transcurrent shear zone, it should be possible to show that significant decrease in metamorphic pressure and temperature occurred during the transition from high grade to low grade ductile mylonites. Aluminous paragneiss within large screens and other, smaller inclusions of supracrustal rocks in the GSLSZ offers the opportunity to determine pressures and temperatures using the garnet–biotite geothermometer (Ferry and Spear, 1978; Hodges and Spear, 1982; St Onge, 1984) and the garnet–plagioclase geobarometer (Newton and Haselton, 1981; Hodges and Spear, 1982; Ganguly and Saxena, 1984; Hodges and Royden, 1984). Spot-analyses were obtained using a Materials Analysis Corporation electron microprobe equipped with a Kevex energy dispersive spectrometer and automated to produce simultaneous multi-element analyses and data reduction (Plant and Lachance, 1973). Operating conditions were as follows: 20 kV accelerating voltage, specimen current of 20 nA measured on standard Kaersutite, and a counting time of 50 s. Standards used are reported in Plant and Lachance (1973).

Field aspects

The full range of metatexite through to homogeneous diatexite structure, as described by Mehnert (1968) and Brown (1973), is present within the paragneiss screens in belts #1 and #2 (Fig. 9a). These migmatites are variably strained. Within a given outcrop, mylonitic to ultramylonitic straight layered gneiss, clearly derived by the tectonic transposition of migmatitic structure, is cross-cut by strongly foliated and tightly folded mature metatexite to inhomogeneous (at outcrop scale) diatexite. This in turn is cross-cut by isotropic homogeneous diatexite containing few misoriented xenoliths of metatexite. No time correlation between outcrops is implied here. However, it is clear that the process of mylonization is both preceded and followed by migmatization (in-situ melt production). This reinforces the contention that the mylonitization of belts #1 and #2 occurred at high metamorphic temperatures, i.e. at temperatures in excess of 625° at $P_{H_2O} = P_{Tot}$ (Piwinski, 1968). In belt #3, the transposed retrograded equivalents of these migmatites form an isolated 5 km long strip along the south shore of Spike Lake (Fig. 3), as well as a number of smaller, isolated inclusions elsewhere within the granitoid mylonites. Samples used in geothermobarometry were taken from Laloche Lake (belt #1), east of Hook Point (belt #2), west of Falls Lake (belt #2) and south of Avocado Lake (belt #3).

Petrography

All samples contain the assemblage garnet–sillimanite–biotite–plagioclase–quartz (Fig. 9b). Cordierite is not uncommon. Minor phases include tourmaline, apatite and mag-ilmenite. Garnets are anhedral, commonly rounded, up to several centimetres in diameter and sporadically contain quartz, sillimanite, plagioclase and biotite as inclusions. They are wrapped by a foliation defined by aligned biotite, sillimanite and ribbon quartz. Sillimanite occurs as acicular to blocky euhedral crystals, generally aligned in the foliation. Biotite forms small irregular to larger euhedral laths. In belt #3, biotite away from the garnets is brown, in contrast to the green biotite closer to, and in textural equilibrium with, the garnets. The green biotite was used for the geothermobarometrical calculations in this case.

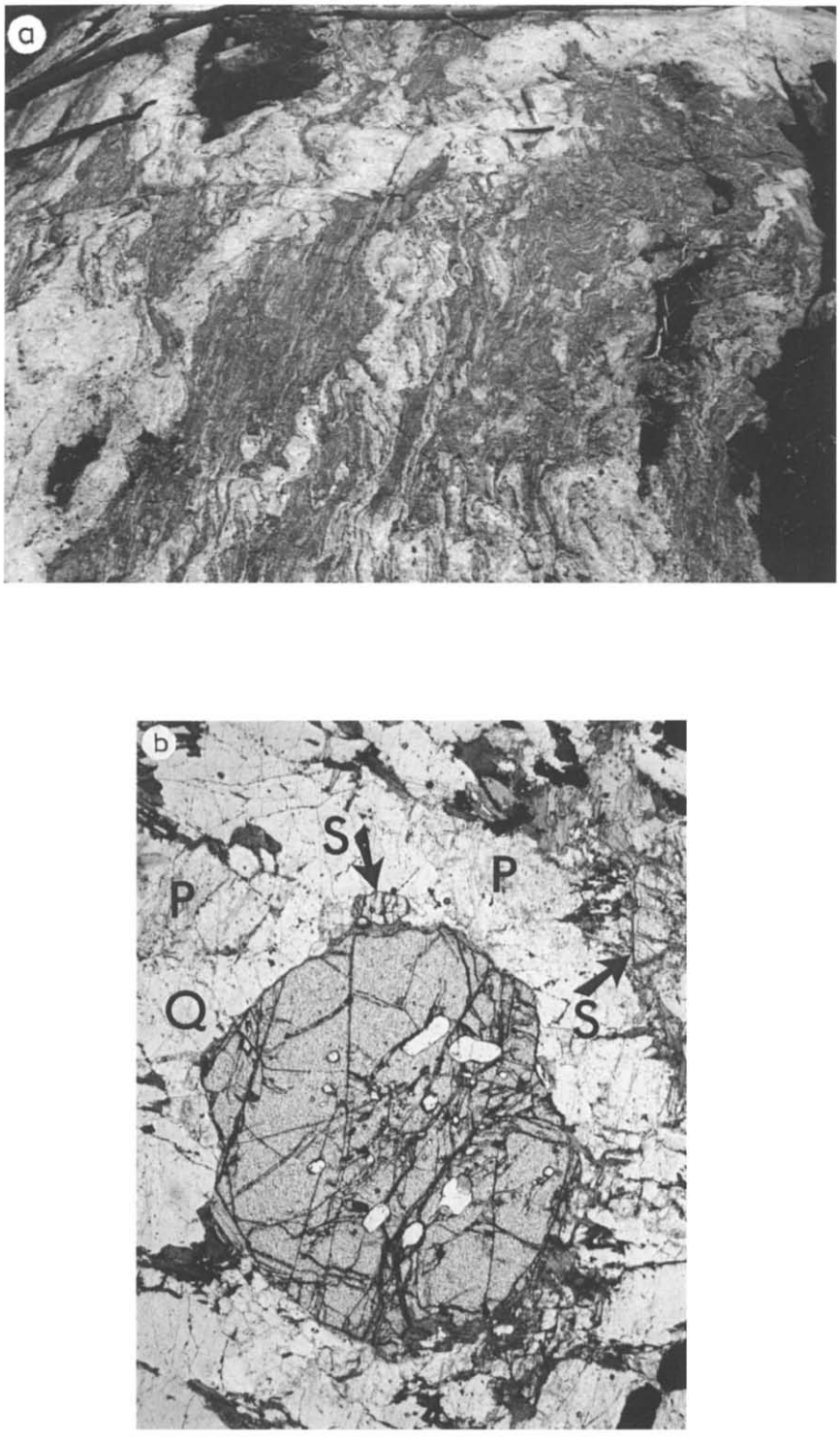

Fig. 9. Material used in geothermobarometry. a. Field aspect of migmatitic aluminous metasediment (metatexite), with abundant foliation parallel stringers of granitic leucosome, cross-cut by isotropic to folded and foliated, coarser grained garnetiferous leucogranite. b. Microscopic aspect of garnet, sillimanite (S), plagioclase (P), quartz (Q) and biotite (dark) in L-47. Quartz inclusions in garnet commonly concentrated in core region. Garnet diameter ca. 2 mm.

Plagioclase occurs as small (2 mm) anhedral grains of homogeneous composition. Quartz is an omnipresent matrix phase.

Results

In most sections, two garnet microstations were analysed. At each garnet microstation up to 20 garnet, 15 matrix plagioclase and 15 matrix biotite spot analyses were made to test for compositional homogeneity. Compositional maps were made of all of the garnets used in this study (Fig. 10). In all samples, care was taken to ensure the presence of an inert phase (quartz or sillimanite) between biotite or plagioclase grains and the adjacent part of the garnet in order to minimize the effect of inter-grain re-equilibration during post-growth cooling. Checks were made to test the effect of separation of matrix phases from the garnet on their composition. Separations of up to one garnet radius (1 mm) revealed no perceptible variation.

The following description applies to samples from belts #1 and #2. Concentric compositional zoning in MgO and FeO is mild, varying by about 2% (mole%) within the range 31–34% for FeO and by just over 1% within the range 5–7% for MgO. There is minimal variation in FeO and MgO from the centre to within 0.1–0.2 times the radius of the rim (Fig. 11). Mg/(Mg + Fe) decreases abruptly within the rim zone, while MnO increases slightly or remains constant and CaO remains constant. Individual garnet spot analyses corresponding to the break in slope of the concentration curves were used in conjunction with spot analyses of matrix phases to calculate pressure and temperature. The average garnet compositions, used in conjunction with average compositions for the matrix phases to calculate the pressures and temperatures presented in Table 1 and Fig. 12, were obtained using spot analyses inboard of the break in slope of the concentration curves. No significant differences were found between the two methods of calculation, as might be expected given

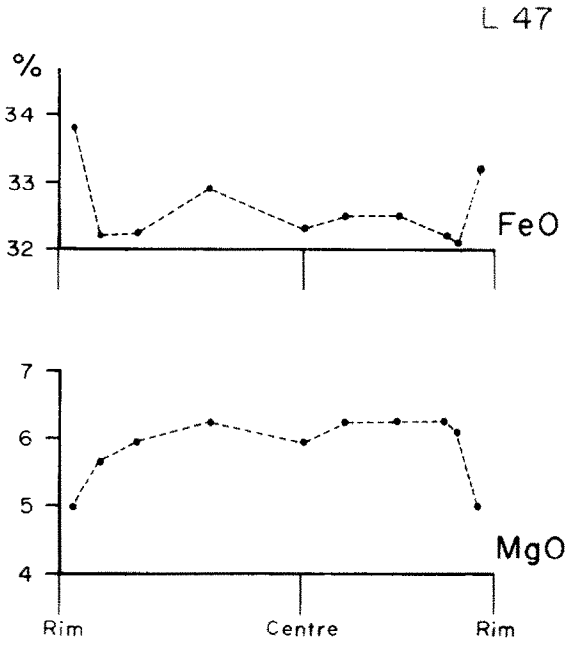

Fig. 11. Mole percentages (%) of FeO and MgO across garnet from L-47 along a rim-to-rim traverse, to illustrate the change in slope of concentration gradients at the rim of the grain. Discussed in text.

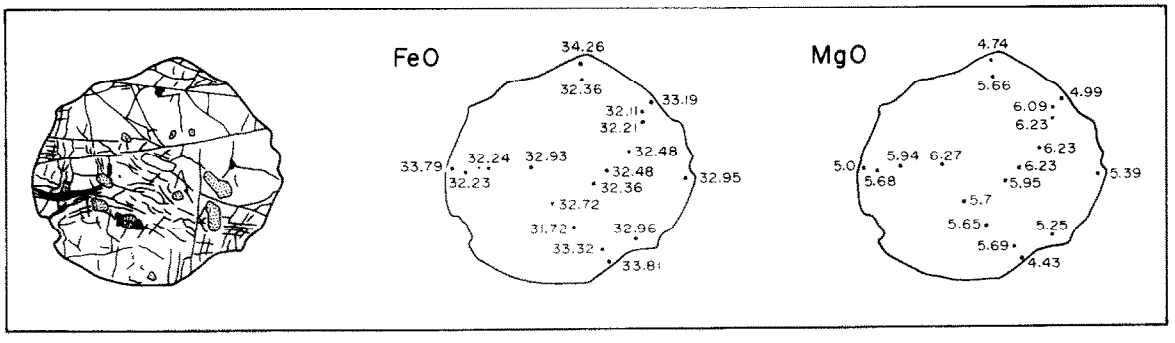

Fig. 10. Maps of FeO and MgO mole percentages (%) in garnet from L-47. Left-hand key-figure drawn from Fig. 9b.

TABLE 1

Averaged microprobe analyses and pressure–temperature results

Sample	Belt	Biotite		Garnet				Plagioclase		
		X.Fe	*X*.Mg	*X*.Fe	*X*.Mg	*X*.Mn	*X*.Ca	*X*.Ca	*P*(Kb)	*T*(C)
L-047	No. 1	0.495	0.505	0.718	0.221	0.021	0.041	0.345	8.2	839
S-619	No. 2	0.566	0.434	0.726	0.188	0.057	0.029	0.326	7.4	895
S-619	No. 2	0.560	0.440	0.704	0.217	0.046	0.032	0.351	7.3	882
S-672	No. 2	0.448	0.552	0.659	0.259	0.048	0.033	0.331	7.8	865
S-576	No. 3	0.537	0.463	0.768	0.142	0.064	0.026	0.287	3.6	652
S-576	No. 3	0.545	0.455	0.769	0.256	0.049	0.026	0.291	4.5	707

the flatness of the concentration curves away from the garnet rims. The distribution of these cation concentrations, coupled with the shapes of the garnets, suggests both constant volume and resorption-associated post-growth diffusion zoning due to inter-grain equilibration with matrix phases (Tracy, 1982). This suggestion was confirmed by analysing biotites in direct contact with garnet:

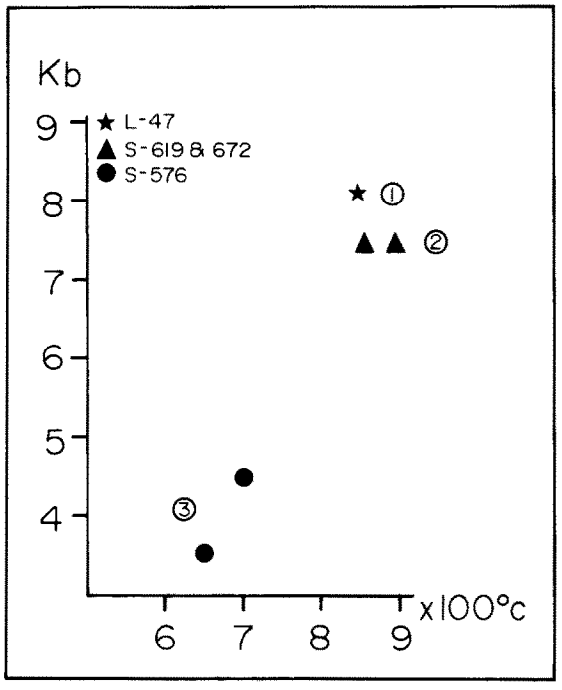

Fig. 12. Geothermobarometry results expressed in $P-T$ space. Circled numbers refer to belts of Great Slave Lake Shear Zone. Maximum preserved pressure and temperature in each belt decrease from belt #1 (oldest) to belt #3 (youngest), with the clearest expression of cooling and decompression between belts #2 and #3. See text.

compared with biotites separated from the garnet by inert phases, MgO is significantly higher (12–13% vs 10%) while FeO is significantly lower (17–18% vs 20%). In biotites, both intra- and inter-grain compositional variation is minimal, within a given thin section. Biotites in belt #1 are distinctly more titaniferous (up to 4%) than those of the other belts. The material from belt #3 differs from the above description in that the garnets are compositionally homogeneous and the brown biotite is more titaniferous and slightly lower in Mg/(Mg + Fe) than the green biotite closer to the garnets.

Maximum preserved temperatures and pressures, estimated using the microprobe analyses of neighbouring biotite, plagioclase and garnet were calculated using the above cited calibrations (Table 1, Fig. 12). Calculated maximum temperatures for both belts #1 and #2 are very high, i.e. close to the maximum stability range of the hornblende which occurs in adjacent granitoid lithologies. Furthermore, the calculated temperatures for belt #2 lie within the granulite field, in apparent contradiction with the observed mineral assemblage. That similar temperatures and pressures were obtained from belt #2 in an independent study by Paul (1986), shows that these are not spurious results. Further work is required to validate these initial results. Emphasizing here the relative values obtained, the following preliminary, though important, conclusions can be drawn from the data. (1) Apparent differences in maximum preserved pressure and temperature between belts #1 and #2 are not significant. On the other hand, the maximum preserved temperatures and pressures

of belt #3 are significantly lower than those of belts #1 and #2. (2) The GSLSZ was undergoing important decompression, presumably associated with uplift and erosion, during relatively high temperature ductile transcurrent shearing. This statement warrants justification. Microstructurally, the sillimanite and biotite are mimetically aligned in the foliation wrapping around both the garnet and larger plagioclases. This suggests that the phases utilized in geothermobarometry were present during the formation of the foliations preserved in each belt. However, it is likely that the compositions of those phases were frozen-in at some time, post-dating the waning of the deformation which generated the foliation. Nevertheless, since the maximum metamorphic conditions recorded from belts #1 and #2 represent a P–T space within which muscovite is unstable, they were frozen-in prior to the establishment of the white mica-bearing foliation in belt #2.

Discussion

The past decade has seen an increase in awareness of the importance of transcurrent faulting in a variety of geological settings in the continental crust. The best studied examples all fall in the elastic-frictional regime (Sibson, 1979) There is wealth of published work on these structures, e.g. Scholz (1977), Crowell (1979), Moore (1979), Sengör (1979), Ricou (1984) and Woodcock (1986). On the other hand, few papers describe in any detail the geology of mature large-scale transcurrent ductile shear zones, the deeper-seated equivalents of the brittle faults. Even an extensive citation list is short: the Cobequid Fault, Nova Scotia (Eisbacher, 1970), the Letlhakane and Palala Shear Zones, Limpopo Belt (Coward et al., 1976; Wakefield, 1977; McCourt and Vearncombe, 1987) the Maydan Shear Zone, Afghanistan (Nicolas et al., 1977), the North and South Armorican Shear Zones, Brittany (Berthé et al., 1979; Watts and Williams, 1979), the Median Tectonic Line, Japan (Hayama and Yamada, 1980, Takagi, 1986), the Northeast Newfoundland Shear Zone (Hanmer, 1981), shear zones in Galicia (Ponce de Leon and Choukroune, 1980), the Coimbra–Cordoba Shear Zone, southern Spain (Burg et al., 1981), the Honam Shear Zone, Korea (Yanai et al., 1986), plus the Greenland examples cited at the beginning of this paper. None of these papers specifically address the question of the evolution of the shear zone anatomy with time, especially as a function of uplift, erosion and consequent decompression. However, the question has been examined in the context of dip and oblique slip faulting (Sibson et al., 1979, 1982; Jamieson, 1986). While the structural contexts are quite different, the geological descriptions given by these authors strongly resemble those presented here, i.e. shear zones cooling and narrowing during decompression.

In a more theoretical vein, the question of the lateral evolution of mature shear zones has recently been raised (Sorensen, 1983; Means, 1984). Do the central parts of shear zones soften or harden with time and, in the latter case, by what process? Sorensen (1983) suggested that shearing was located in the lateral walls of shear zones which migrate away from the stiffening central parts of the zone. Few authors have attempted dynamic analysis of large-scale shear zones (Watterson, 1979; Sorensen, 1983). Even fewer papers have dealt with the question of the initiation of large-scale ductile shear zones (Watterson, 1979; regarding small-scale shear zones see Simpson, 1983; Segall and Simpson, 1986; Ingles, 1986). It is unlikely that large-scale shear zones initiate as parallel-sided corridors of longitudinally homogeneous strain (Mandl, 1987). They probably comprise three-dimensionally braided zones of higher strain anastomosing around islands of lower strain, i.e. a mesh-structure (Sibson, 1979, 1986; see also Bell, 1981; Bell and Hammond, 1984). At maturity, the initially stiff material of the islands of lower strain has been incorporated into the mylonite by dynamic strain softening.

It is significant that mature large-scale greenschist facies mylonite zones do not exceed 1–2 km in width, and most often are less than 1 km wide e.g. the Laloche River belt and Hornby Channel belt (this study), the South Armorican Shear Zone, Brittany (Berthé et al., 1979), the Dover Fault, Newfoundland (Hanmer, 1981), the Median Tectonic Line, Japan (Takagi, 1986), the

Merens Fault, Pyrenees (Carreras and Cirés, 1986), to cite but transcurrent examples. I suggest that this represents the minimum width of mylonitic corridor required, for the given metamorphic conditions, to (1) accommodate natural imposed displacement rates at the slowest, geologically reasonable strain rates (Pfiffner and Ramsay, 1982) and perhaps (2) ensure that mechanical interference between wall rock asperities and the fault rock is at a minimum. If the first suggestion is valid, then I would propose that it applies to all large-scale transcurrent ductile shear zones, under all solid-state, crustal metamorphic conditions. Obviously, all other factors being equal, the higher the metamorphic temperature, the wider the shear zone and the slower the minimum strain rate possible. It is beyond the scope of this paper to attempt to estimate the sensitivity of shear zone width to variation in displacement rate; however, from the example of the GSLSZ, mature shear zones may change width and migrate laterally as a function of thermally activated rheological change within the wall rocks. Under appropriate conditions, similar rheological change could also be hydrolytically controlled.

In the GSLSZ, cooling was accompanied by uplift, erosion and consequent decompression. This raises an important regional tectonic problem concerning the cause of uplift of an active transcurrent structure. Suffice it to say here that the GSLSZ appears to have acted initially as a transcurrent, and later as a transform fault during convergence and initial collision of the Slave Craton with the Churchill Province, with the GSLSZ sited on the Churchill plate (Hoffman et al., 1986; Hoffman, 1987). Eastward-directed subduction below the Churchill plate throughout convergence and initial collision, as proposed by these authors, might tentatively be looked to as a potential cause of progressive uplift of the active transcurrent GSLSZ.

Conclusions

The Great Slave Lake Shear Zone (GSLSZ) of the northwestern Canadian Shield, one of the widest (25 km) documented mylonite zones in the world to date, is a type example of the crustal-scale fault profile. With time, the metamorphic grade of the present erosion level decreased from granulite to greenschist facies. The locus of high strain narrowed and jumped laterally to abandon once active older mylonites. Progressively younger mylonites represent both cooler temperatures and lower pressures. Thus the sequence of narrowing mylonite belts is interpreted to represent a series of progressively shallower seated sections through the GSLSZ. Deformation evolved through the brittle–ductile transition, initially producing non-dilational penetrative breccias, followed by discrete non-dilational faulting and finally long dilational quartz "stockworks".

More generally, developing crustal-scale shear zones appear to grow to an optimum width dictated by the requirement of attaining the slowest, geologically reasonable strain rates for given conditions of wall rock rheology and displacement rate. Independently of change in relative plate motions, mature shear zones should change width and migrate laterally as a function of thermally activated rheological change within the wall rocks.

Acknowledgements

I have benefited greatly from discussions with colleagues at the Geological Survey of Canada. I am especially indebted to Marc St-Onge and John Percival for patiently guiding me, uninitiated, through the geothermobarometrical gauntlet. Discussions with Paul Hoffman and Robert Hildebrand have placed my structural work into a tectonic framework. Fieldwork at Great Slave Lake was enthusiastically shared by my senior assistants Steve Lucas and Jim Connelly, and my work on the microprobe was only possible thanks to Morizio Bonardi and Gina Lecheminant. I thank Cees Van Staal, Marc St-Onge and Robert Hildebrand for thoughtful and thorough reviews of the original manuscript. I am also indebted to Russel Black and Shin Ichi Yoshikura for bringing the Ubendian and Honam structures to my attention. All errors of interpretation are, of course, my own. This is Geological Survey of Canada Contribution #34087.

References

Bak, J., Korstgard, J.A. and Sorensen, K., 1975a. A major shear zone within the Nagssugtoquidian of West Greenland. Tectonophysics, 27: 191–209.

Bak, J., Sorensen, K., Grocott, J., Korstgard, J.A., Nash, D. and Watterson, J., 1975b. Tectonic implications of Precambrian shear belts in Western Greenland. Nature, 254: 566–569.

Bell, T.H., 1981. Foliation development—the contribution, geometry and significance of progressive, bulk, inhomogeneous shortening. Tectonophysics, 75: 273–296.

Bell, T.H. and Etheridge, M.A., 1973. Microstructures of mylonites and their descriptive terminology. Lithos, 6: 337–348.

Bell, T.H. and Hammond, R.L., 1984. On the internal geometry of mylonite zones. J. Geol., 92: 667–686.

Berthé, D., Choukroune, P. and Jegouzo, P., 1979. Orthogneiss, mylonite and non-coaxial deformation of granites: the example of the South Armorican shear zone. J. Struct. Geol., 1: 31–42.

Bostock, H.H., 1982. Geology of the Fort Smith map area. Northwestern Territories (NTS 75D). Geol. Surv. Can. Open File, 859, 52 pp.

Bostock, H.H., 1987. Geology of the south half of the taltson Lake map area, District of Mackenzie. In: Current Research. Geol. Surv. Can., Pap., 87–1A: 443–450.

Bostock, H.H., van Breemen, O. and Loveridge, W.D., 1987. Proterozoic geochronology in the Taltson Magmatic Zone, NWT. Geol. Surv. Can., Pap., 87–2: 73–80.

Brown, M., 1973. The definition of metatexis, diatexis and migmatite. Proc. Geol. Assoc., 84: 371–382.

Burg, J.P., Iglesias, M., Laurent, P., Matte, P. and Ribeiro, A., 1981. Variscan intracontinental deformation: the Coimbra–Cordoba shear zone (SW Iberian Peninsula). Tectonophysics, 78: 161–177.

Carreras, J. and Cires, J., 1986. The geological significance of the western termination of the Merens Fault in Port Vell (Central Pyrenees). Tectonophysics, 129: 99–114.

Coward, M.P., 1984. Major shear zones in the precambrian crust: examples from NW Scotland and Southern Africa. In: A. Kröner and R. Greiling (Editors), Precambrian Tectonics Illustrated. Schweitzerbart, Stuttgart, pp. 207–235.

Coward, M.P., James, P.R. and Wright, L.I., 1976. The movement pattern across the northern margin of the Limpopo mobile belt, southern Africa. Geol. Soc. Am. Bull., 87: 601–611.

Crowell, J.C., 1979. The San Andreas Fault System through time. J. Geol. Soc. London, 136: 293–302.

Davidson, A., 1984. Identification of ductile shear zones in the southwestern Grenville Province of the Canadian Shield. In: A. Kröner and R. Greiling (Editors), Precambrian Tectonics Illustrated. Schweitzerbart, Stuttgart, pp. 207–235.

Durney, D.W. and Ramsay, J.G., 1973. Incremental strains measured by syntectonic crystal growths. In: K.A. De Jong and R. Scholten (Editors), Gravity and Tectonics. Wiley, New York, 502 pp.

Eisbacher, G.H., 1970. Deformation mechanisms of mylonitic rocks and fractured granites in the Cobequid Mountains, Nova Scotia, Canada. Geol. Soc. Am. Bull., 81: 2009–2020.

Ferry, J.M. and Spear, F.S., 1978. Experimental calibration of the partitioning of Fe and Mg between biotite and garnet. Contrib. Miner. Petrol., 66: 113–117.

Ganguly, J. and Saxena, S.K., 1984. Mixing properties of aluminosilicate garnets: cosntraints from natural and experimental data and applications to geothermo-barometry. Am. Mineral., 69: 88–97.

Geological Survey of Canada, 1964a. Taltson Lake, District of Mackenzie, NWT. Geol. Surv. Can., Map 7184G.

Geological Survey of Canada, 1964b. Snowdrift, District of Mackenzie, NWT. Geol. Surv. Can., Map 7189G.

Geological Survey of Canada, 1984. Lockhart River, NWT. Geol. Surv. Can., Map 1566-A.

Grocott, J., 1977. The relationship between Precambrian shear belts and modern fault systems. J. Geol. Soc. London, 133: 257–262.

Grocott, J., 1979a. Controls of metamorphic grade in shear belts. Rapp. Grønlands Geol. Unders., 89: 47–62.

Grocott, J., 1979b. Shape fabrics and superimposed simple shear strain in a Precambrian shear belt, W. Greenland. J. Geol. Soc. London, 136: 471–488.

Grocott, J., 1981. Fracture geometry of pseudotachylite generation zones: a study of shear fractures formed during seismic events. J. Struct. Geol. 3: 169–178.

Grocott, J. and Watterson, J., 1980. Strain profile of a boundary within a large ductile shear zone. J. Struct. Geol., 2: 111–118.

Hanmer, S., 1981. Tectonic significance of the northeastern Gander Zone, Newfoundland: an Acadian ductile shear zone. Can. J. Earth Sci., 18: 120–135.

Hanmer, S., 1984. The potential use of planar and elliptical structures as indicators of strain regime and kinematics of tectonic flow. Geol. Surv. Can., Pap. 84-1B: 133–142.

Hanmer, S., 1986. Asymmetrical pull-aparts and foliation fish as kinematic indicators. J. Struct. Geol., 8: 111–122.

Hanmer, S., 1987. Textural map-units in quartzofeldspathic mylonitic rocks. Can. J. Earth Sci. 24: 2065–2073.

Hanmer, S. and Connelly, J.N., 1986. Mechanical role of the syntectonic Laloche Batholith in the Great Slave Lake Shear Zone, District of Mackenzie, NWT. In: Current Research. Geol. Surv. Can., Pap., 86-1B: 811–826.

Hanmer, S. and Lucas, S.B., 1985. Anatomy of a ductile transcurrent shear: the Great Slave Lake Shear Zone, District of Mackenzie, NWT (preliminary report). Geol. Surv. Can., Pap., 85-1B: 7–22.

Hayama, Y. and Yamada, T., 1980. Median Tectonic Line at the stage of its origin in relation to plutonism and mylonitisation in the Ryoke Belt. Mem. Geol. Soc. Jpn., 18: 5–26.

Henderson, J.F., 1939. Taltson Lake, District of Mackenzie, NWT. Geol. Surv. Can., Map, 525A.

Hodges, K.V. and Royden, L., 1984. Geologic thermobarometry of retrograded metamorphic rocks: an indication of the uplift trajectory of a portion of the northern Scandinavian Caledonides. J. Geophys. Res., 89: 7077–7090.

Hodges, K.V. and Spear, F.S, 1982. Geothermometry, geobarometry and the Al_2SiO_5 triple point at Mt Moosilauke, New Hampshire. Am. Mineral., 67: 1118–1134.

Hoffman, P.F., 1987. Continental transform tectonics: Great Slave Lake shear zone (ca 1.9 Ga), northwest Canada. Geology., 15: 785–788.

Hoffman, P.F., Bell, I.R., Hildebrand, R.S. and Thorstad, L., 1977. Geology of the Athapuscow Aulacogen, East Arm of Great Slave Lake, District of Mackenzie. Geol. Surv. Pap., 77–1A: 117–129.

Hoffman, P.F., Culshaw, N.G., Hanmer, S., Lecheminant, A.N., McGrath, P.H., Tirrul, R., van Breemen, O., Bowring, S.A. and Grotzinger, J.P., 1986. Is the Thelon Front (NWT) a suture? GAC–MAC Joint Annu. Meet., Progr. Abstr., p. 82.

Ingles, J., 1986. Terminations of ductile shear zones. Tectonophysics, 127: 87–95.

Jamieson, R.A., 1986. $P-T$ paths from high temperature shear zones beneath ophiolites. J. Metamorph. Geol., 4: 3–22.

Lachenbruch, A.H. and Sass, J.H., 1980. Heat flow and energetics of the San Andreas Fault Zone. J. Geophys. Res., 85: 6185–6222.

Mandl, G., 1987. Discontinuous fault zones. J. Struct. Geol., 9: 105–110.

McCourt, S. and Vearncombe, J.R., 1987. Shear zones bounding the central zone of the Limpopo Mobile Belt, southern Africa. J. Struct. Geol., 9: 127–138.

Means, W.D., 1984. Shear zones of types I and II and their significance for reconstruction of rock history. Ged. Soc. Am., NE Sect. Annu. Meet., Prog. Abstr., p. 50.

Mehnert, K.R., 1968. Migmatites and the Origin of Granitic Rocks. Elsevier, Amsterdam, 405 pp.

Moore, J. McM., 1979. Tectonics of the Najd transcurrent fault system, Saudi Arabia. J. Geol. Soc. London, 136: 441–454.

Murphy, D.C., 1987. Superstructure/infrastructure transition, east-central Cariboo Mountains, British Columbia: geometry, kinematics and tectonic implications. J. Struct. Geol., 9: 13–30.

Myers, J.S., 1978. Formation of banded gneisses by deformation of igneous rocks. Precam. Res., 6: 43–64.

Myers, J.S, 1984. Archaean tectonics in the Fiskenaesset region of southwest Greenland. In: A. Kröner and R. Greiling (Editors), Precambrian Tectonics Illustrated. Schweitzerbart, Stuttgart, pp. 95–112.

Newton, R.C. and Haselton, H.T., 1981. Thermodynamics of the garnet–plagioclase–Al_2SiO_5–quartz geobarometer. In: R.C. Newton, A. Navrotsky and B.J. Wood (Editors), Thermodynamics of Minerals and Melts. Springer, New York, pp. 131–147.

Nicolas, A., Bouchez, J.L., Blaise, J. and Poirier, J.P., 1977. Geological aspects of deformation in continental shear zones. Tectonophysics, 42: 55–73.

Nicolas, A. and Poirier, J.P., 1976. Crystalline Plasticity and Solid State Flow in Metamorphic Rocks. Wiley, New York, 444 pp.

Passchier, C.W. and Simpson, C., 1986. Porphyroclast systems as kinematic indicators. J. Struct. Geol., 8: 831–844.

Paterson, M.S., 1978. Experimental Rock Deformation: the Brittle Field. Springer, New York, 254 pp.

Paul, D., 1986. Geothermometry and geobarometry of pelitic gneisses in the Great Slave Lake Shear Zone, NWT. Unpublished Thesis, Ottawa Univ., 39 pp.

Pfiffner, O.A. and Ramsay, J.G., 1982. Constraints on geological strain rates: arguments from finite strain states of naturally deformed rocks. J. Geophys. Res., 87: 311–321.

Piwinski, A.J., 1968. Experimental studies of igneous rock series, central Sierra Nevada Batholith, California. J. Geol., 76: 548–570.

Plant, A.G. and Lachance, G.R., 1973. Quantitative electron microprobe analysis using an energy dispersive spectrometer. Proc. 8th Nat. Conf. on Electron Probe Analysis, Pap. 13.

Poirier, J.P., 1985. Creep of Crystals: High-temperature Deformation Processes in Metals, Ceramics and Minerals. University Press, Cambridge, 260 pp.

Poirier, J.P. and Guillopé, M., 1979. Deformation induced recrystallisation of minerals. Bull. Minéral., 102: 67–74.

Ponce de Leon, M. and Choukroune, P., 1980. Shear zones in the Iberian Arc. J. Struct. Geol., 2: 63–68.

Ramsay, J.G. and Graham, R.H., 1970. Strain variation in shear belts. Can. J. Earth Sci., 7: 786–813.

Reinhardt, E.W., 1969. Geology of the precambrian rocks of Thubun Lakes map area in relationship to the McDonald Fault system, District of Mackenzie (75E/12 and parts of 75E/13 and 85H/9). Geol. Surv. Can., Pap., 69–21: 29 pp.

Ricou, L.E., 1984. Les Alpes Occidentales: chaîne de déchrochement. Bull. Soc. Géol. Fr., 26: 861–874.

St-Onge, M.R., 1984. Geothermometry and geobarometry in pelitic rocks of north-central Wopmay Orogen (early Proterozoic), Northwestern Territories, Canada. Geol. Soc. Am. Bull., 95: 196–208.

Sanderson, D.J. and Marchini, R.D., 1984. Transpression. J. Struct. Geol., 6: 449–549.

Scholtz, C.H., 1977. Transform fault systems of California and New Zealand: similarities in their tectonic and seismic styles. J. Geol. Soc. London, 133: 215–229.

Segall, P. and Simpson, C., 1986. Nucleation of ductile shear zones on dilatant fractures. Geology, 14: 56–59.

Sengör, A.M.C., 1979. The North Anatolian transform fault: its age, offset and tectonic significance. J. Geol. Soc. London, 136: 269–282.

Sibson, R.H., 1977. Fault rocks and fault mechanisms. J. Geol. Soc. London, 133: 191–213.

Sibson, R.H., 1979. Fault rocks and structure as indicators of shallow earthquake source processes. U.S. Geol. Surv. Open File Rep., 79/1239: 276–304.

Sibson, R.H., 1982. Fault zone models, heat flow and the depth distribution of earthquakes in the continental crust of the United States. Seismol. Soc. Am. Bull., 72: 151–163.

Sibson, R.H., 1983. Continental fault structure and the shallow earthquake source. J. Geol. Soc. London, 140: 741–767.

Sibson, R.H., 1986. Earthquakes and rock deformation in crustal fault zones. Ann. Rev. Earth Planet. Sci., 14: 149–175.

Sibson, R.H., White, S.H. and Atkinson, B.K., 1979. Fault rock distribution and structure within the Alpine Fault Zone: a preliminary account. R. Soc. N. Z. Bull., 18: 55–65.

Sibson, R.H., White, S.H. and Atkinson, B.K., 1981. Structure and distribution of fault rocks in the Alpine Fault Zone, New Zealand. Geol. Soc. London, Spec. Publ., No. 9, pp. 197–210.

Simpson, C., 1983. Displacement and strain patterns from naturally occurring shear zone terminations. J. Struct. Geol., 5: 497–506.

Sorensen, K., 1983. Growth dynamics of the Nordre Stromfjord Shear Zone. J. Geophys. Res., 88: 3419–3437.

Stockwell, C.H., 1932. Great Slave Lake–Coppermine River area, NWT. Geol. Surv. Summary Rep., Pt C, pp. 37–63.

Strekeisen, A.L., 1976. To each plutonic rock its proper name. Earth Sci. Rev., 12: 1–33.

Takagi, H., 1986. Implications of mylonitic microstructures for the geotectonic evolution of the Median Tectonic Line, central Japan. J. Struct. Geol., 8: 3–14.

Thompson, P.H., Culshaw, N.G., Thompson, D.L. and Buchanan, J.R., 1985. Geology across the western boundary of the Thelon Tectonic Zone in the Tinney Hills–Overby Lake (West Half) map area, District of Mackenzie. In: Current Research, Pt A. Geol. Surv. Can., Pap., 85-1A: 555–572.

Tracy, R.J., 1982. Compositional zoning and inclusions in metamorphic minerals. In: J.M. Ferry (Editor), Miner. Soc. Am., Rev. Mineral., 10: 355–397.

Tullis, J. and Yund, R.A., 1977. Experimental deformation of dry Westerly Granite. J. Struct. Geol., 82: 5705–5718.

Tullis, J. and Yund, R.A., 1980. Hydrolytic weakening of experimentally deformed Westerly Granite and Hale albite rock. J. Struct. Geol., 2: 439–453.

Wakefield, J., 1977. Mylonitisation in the Lethakane shear zone, eastern Botswana. J. Geol. Soc. London, 133: 263–275.

Watterson, J., 1975. Mechanism for the persistence of tectonic lineaments. Nature, 253: 520–521.

Watterson, J., 1979. Strain and strain rate gradients of the ductile levels of fault displacements. U.S. Geol. Surv., Open File Rep., 79-1239: 235–257.

Watts, M.J. and Williams, G.D., 1979. Fault rocks as indicators of progressive shear deformation in the Guingamp region, Brittany. J. Struct. Geol., 1: 323–332.

White, S.H., 1976. The effects of strain on microstructures, fabrics and deformation mechanisms in quartzites. Philos. Trans. R. Soc. London, Ser. A, 283: 69–86.

White, S.H., Burrows, S.E., Carreras, J., Shaw, N.D. and Humphreys, F.J., 1980. On mylonites in ductile shear zones. J. Struct. Geol., 2: 175–187.

White, S. and Knipe, R.J., 1978. Transformation and reaction enhanced ductility in rocks. J. Geol. Soc. Londen, 135: 513–516.

Williams, G.D. and Dixon, J., 1982. Reaction and geometrical softening in granitoid mylonites. Textures Microstruct., 4: 223–239.

Woodcock, N.H., 1986. The role of strike-slip fault systems at plate boundaries. Phil. Trans. R. Soc. London, Ser. A, 317: 13–29.

Wright, G.M., 1951. Second preliminary map, Christie Bay, District of Mackenzie, NWT. Geol. Surv. Can., Pap. 57–25.

Wright, G.M., 1952. Second preliminary map, Reliance, District of Mackenzie, NWT. Geol. Surv. Can., Pap. 51–26.

Yanai, S., Park, B. and Otoh, S., 1986. The Honam Shear Zone (South Korea): deformation and tectonic implication in the Far East. Sci. Pap., Univ. Tokyo, 35: 181–209.